

Carbon isotopic composition and its implications on paleoclimate of the underground ancient forest ecosystem in Sihui, Guangdong

DING Ping^{1,2}, SHEN ChengDe^{1,3†}, WANG Ning^{1,2}, YI WeiXi¹, LIU KeXin³, DING XingFang³ & FU DongPo³

¹ Key Laboratory of Isotope Geochronology and Geochemistry, Guangzhou Institute of Geochemistry, Chinese Academy of Sciences, Guangzhou 510640, China;

² Graduate University of Chinese Academy of Sciences, Beijing 100049, China;

³ Key Laboratory of Heavy Ion Physics, Peking University, Beijing 100871, China

We present the carbon isotopic composition of the total organic carbon (TOC) and fine roots in the sedimentary profile from the underground ancient forest in Sihui to study the climatic and environmental changes from 4.5 ka BP to 0.6 ka BP. Results show that C₃ plant was the main vegetation from 4.5 ka BP to 0.6 ka BP in this region. The ancient forest began to develop in the wetland at around 4 ka BP and disappeared together with the wetland at about 3.0 ka BP, implying that the climate had changed greatly at around 3.0 ka BP. As indicated by the simulation results, the content of atmospheric CO₂ increased slightly during 3.5 ka BP and 3.0 ka BP, implying climate warming during that period. The interval of radiocarbon age between 3.0 ka BP and 1.2 ka BP was possibly caused by the strong erosion when the block was lifted in the neotectonic movement. From 1.2 ka BP to 0.6 ka BP, the region remained in terrestrial sedimentary environment, and the surface plant biomass declined gradually. Drought caused by the climate change was the likely cause for the disappearance of the ancient forest. South transition of Intertropical Convergence Zone (ITCZ) was probably the main mechanism for the climate change.

Holocene, underground ancient forest, Pearl River Delta, fine root, atmospheric CO₂

Studying climate variation of Holocene helps us better understand the relationship between human activities and natural factors^[1–6]. At present, researches on the climate change of Holocene in China concentrate on three periods^[7–10]: the early Holocene with temperature climbing, warm period in the middle Holocene, and the late Holocene with temperature decreasing. Results from the lake and cave sediments in the low latitude regions around the world showed that the climate turned cold and dry with a sharp decrease in precipitation from 3.2 ka BP to 2.7 ka BP^[1,11–13]. This event may have greatly changed the ecosystem and activities of human in Pearl River Delta. It may be also one of the reasons for the termination of the Shell Mound Sites and Sand Mound Sites.

Many ancient forests were found in Sihui, and the dominate tree species was hydrophilous plant *Glyptostrobus pensilis*. The evolutionary history of the ancient forests offers us an important way to reconstruct the climate and geographical environment of Pearl River Delta. However, we still know little about the chronostratigraphy of the ancient forests and their indications on paleoclimate. Li et al.^[14] has first studied the ancient

Received November 23, 2007; accepted September 9, 2008; published online February 20, 2009

doi: 10.1007/s11430-009-0014-2

†Corresponding author (email: cdshen@gig.ac.cn)

Supported by National Natural Science Foundation of China (Grant Nos. 40231015 and 40473002), National Basic Research Program of China (Grant No. 2005CB422004), the Knowledge Innovation Program of the Chinese Academy of Sciences (Grant No. KSCX2-SW-133) and Open Funds of State Key Laboratory of Organic Geochemistry (Grant No. OGL-200607)

timbers buried under Pearl River Delta, and considered that the death of the timbers was associated with the Litter Ice Age. Recent study has suggested that over-cutting by the ancient people was probably one of the reasons for the death of the ancient timbers^[15].

In this paper, we try to decipher the evolutionary history of the climate and geographical environment from 4.5 ka BP to 0.6 ka BP based on the content of TOC, the carbon isotopes of TOC, and fine roots. We also discuss the mechanism for the climatic and environmental changes and their impact on the human activities.

1 Sampling and method

The sedimentary profile of the ancient forest is located in Longfu, the central part of Sihui, Guangdong Province. It also lies in the northwest of Pearl River Delta and lower reaches of Xijiang River, Beijiang River and

Suihe River. The geographic location is 23°22'359"N and 112°42'497"E. The geography of Sihui is characterized by mountains in the north and west, alluvial plains in the south and east, and hills and valley basin in the central (Figure 1). Current mean annual temperature (MAT) is 21°C, and main annual precipitation (MAP) is 1800 mm in the region. It belongs to subtropical monsoon climate and is strongly influenced by East Asian Monsoon. The subtropical monsoon evergreen broadleaf forest is the main vegetation.

The sedimentary profile is 4.8 m high, and consists of 4 layers with clear boundary lines: the coarse aleuritic clay layer (layer A), the fine aleuritic clay layer (layer B), the humic layer (layer C) and the aleuritic clay layer (layer D). Sampling interval in layers C and D is 20 cm. Detailed distributions of the sampling sites in layers A and B are showed in Figure 2.

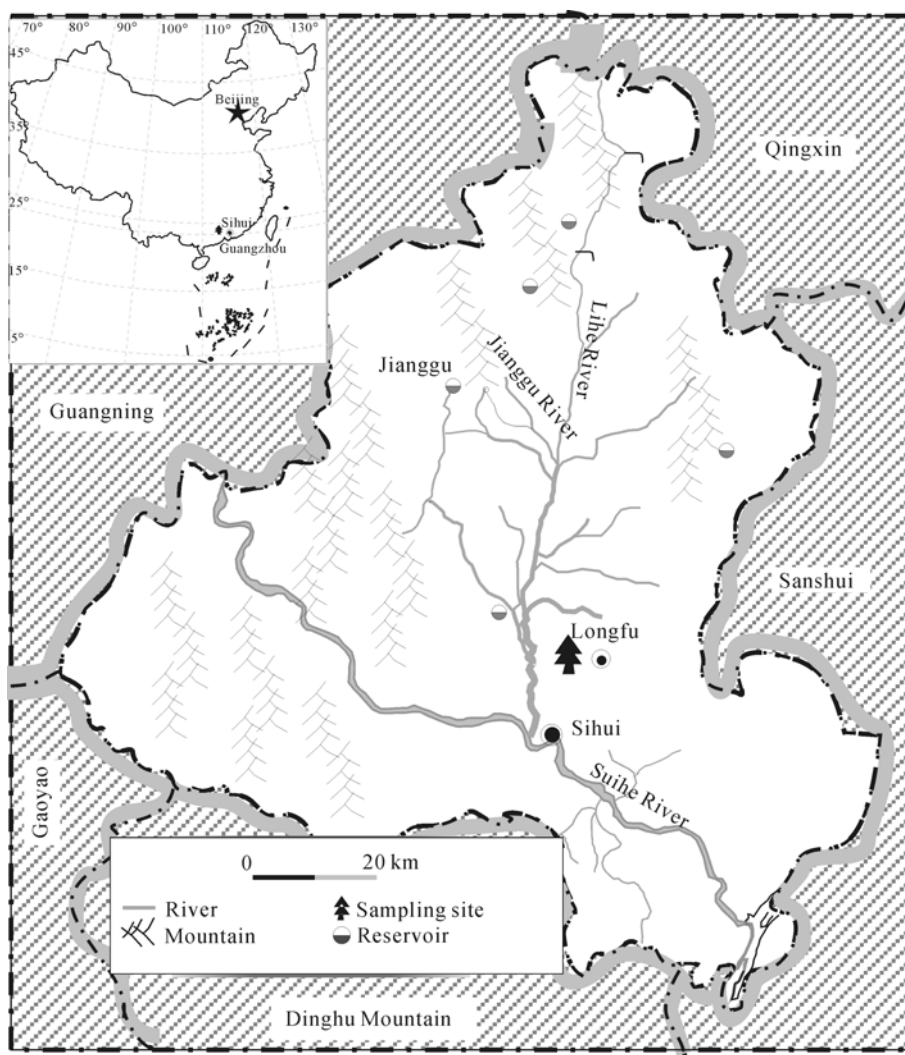


Figure 1 Location map of the sampling site, denoted by tree sign.

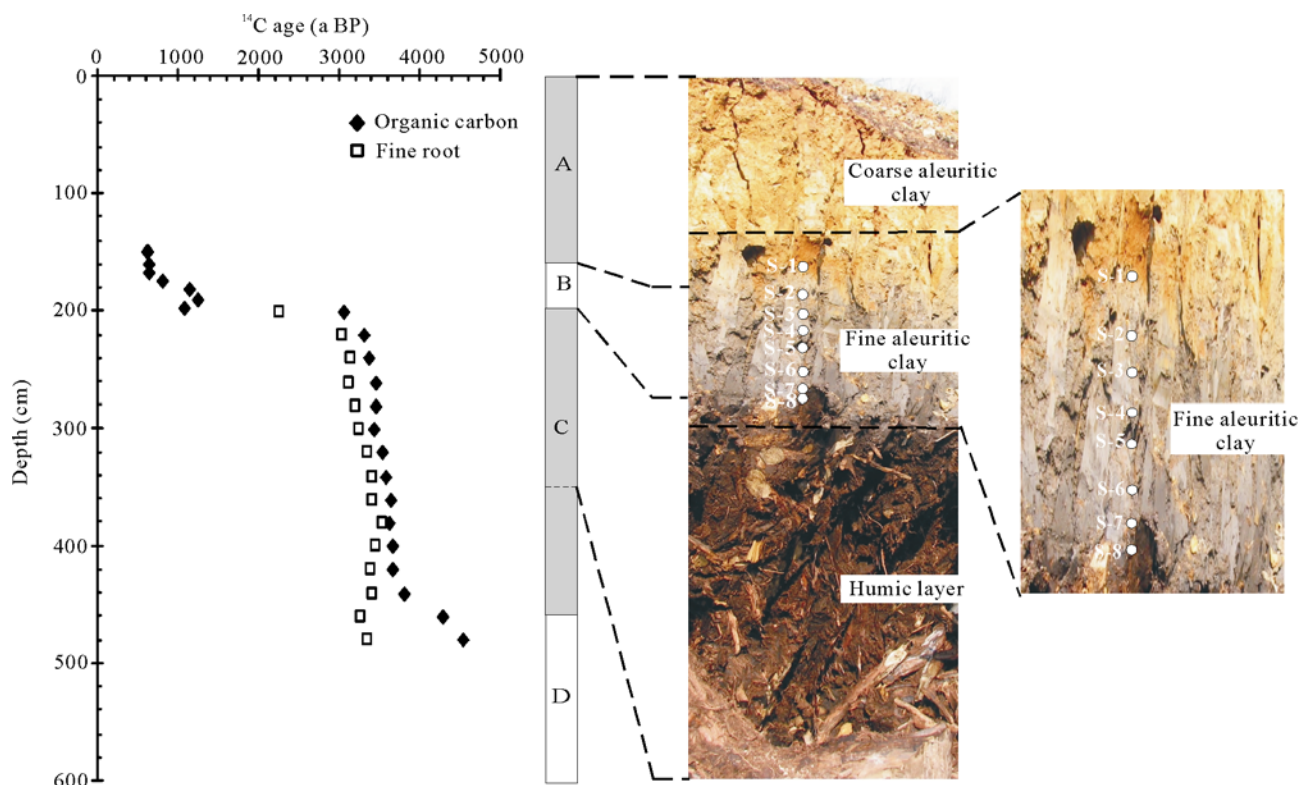


Figure 2 Radiocarbon chronostratigraphy and distributions of the sampling sites in layers A and B.

For the method for the preparation of fine root^[15]. All the preparations of sediments and fine roots were carried out at the AMS-¹⁴C laboratory in the Key Laboratory of Isotope Geochronology and Geochemistry, Chinese Academy of Sciences (CAS). The $\delta^{13}\text{C}$ values of CO_2 transformed from TOC were measured by Finigan Model-251 isotopic ratio mass spectrometer facility (PDB standard) with a precision of $\pm 0.02\text{‰}$ at the State Key Laboratory of Loess and Quaternary Geology. Graphite targets for ¹⁴C dating were measured at the Key Laboratory of Heavy Ion Physics, Peking University, AMS facility. The contents of TOC were determined by a microbarograph in the vacuum system in our laboratory.

2 Results and discussion

2.1 Distribution of $\delta^{13}\text{C}$ values in the sedimentary profile

Changes of $\delta^{13}\text{C}$ values can reflect the variation of the plant types and the decomposition state of the organic carbon^[16,17], which is expressed by $\delta^{13}\text{C} = \left(\frac{^{13}\text{C}/^{12}\text{C}}{^{13}\text{C}/^{12}\text{C}}_{\text{standard}} - 1 \right) \times 1000\text{‰}$. Based on the different pathways of photosynthesis, the plant can be divided into three different types: C_3 , C_4 and CAM. Each type

has a different range of $\delta^{13}\text{C}$ values: -34‰ — -23‰ for C_3 plant, -22‰ — -6‰ for C_4 plant, and -20‰ — -10‰ for CAM plant^[18]. In the sedimentary profile, the $\delta^{13}\text{C}$ values varied between -29.85‰ and -25.58‰ , all falling in the range of C_3 plant, suggesting that the main vegetation was C_3 plant from 4.5 ka BP to 0.6 ka BP in this region.

Figure 3 shows that the $\delta^{13}\text{C}$ values increased with the depth exponentially from -28.99‰ to -25.58‰ in the layers A and B, exhibiting a variation of 3.4‰, which was likely caused by the fractionation when the organic carbon was decomposed. Plant change may also lead to the variation of $\delta^{13}\text{C}$ values, which is revealed by the great fluctuation of the $\delta^{13}\text{C}$ values of the sediments^[19]. However, the $\delta^{13}\text{C}$ values in layers A and B had not exhibited such a fluctuation. Therefore, the variation of the $\delta^{13}\text{C}$ values in layers A and B only reflected the decomposition degree of the organic carbon.

Given the precision of modern mass spectrograph ($\pm 0.02\text{‰}$) and the error produced during the sample preparation ($\pm 0.2\text{‰}$), the $\delta^{13}\text{C}$ values remained stable in layer C: -29.04‰ and -29.85‰ , suggesting that the organic carbon almost remained undecomposed, and the

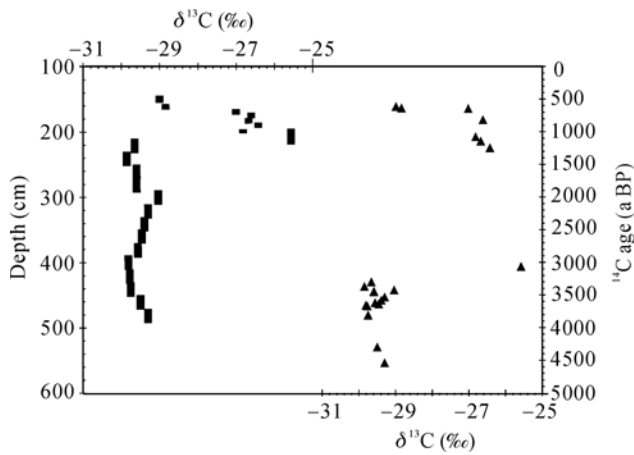


Figure 3 Variation of $\delta^{13}\text{C}$ values with depth and age in the sedimentary profile.

sedimentary environment kept reductive from 3813 ± 31 a BP to 3068 ± 35 a BP. Similar to layer C, the $\delta^{13}\text{C}$ values in layer D ranged from -29.5‰ to -29.3‰ , indicating that the organic carbon may partly come from layer C. The obvious distinction of the $\delta^{13}\text{C}$ values among layers A, B, and C implied that great ecological change happened around 3.0 ka BP, which finally led to the disappearance of the original ecosystem.

2.2 Distribution of TOC in the sedimentary profile

Contrary to decreasing with age and depth in the typical soil profile^[20,21], the content of TOC increased exponentially from 0.8% to 5.5% in layers A and B (Figure 4(a) and (b)). Two causes may be responsible for it: 1) The amount of organic matters entering the layers A and B declined with time; 2) Organic matters in layers A and B were partly transferred from layer C. However, a 4.0‰ variation of the $\delta^{13}\text{C}$ values between the bottom of layer B and layer C suggested that the organic matters could not come from layer C. Therefore, the organic matters in layers A and B were from the surface soil of the surroundings, and the variation of the content of TOC stood for the change of the vegetation density, which suggested that the biomass of the surface vegetation had a decreasing tendency from 1.2 ka BP to 0.6 ka BP in this region.

Layer C in which the ancient forest developed had the ^{14}C chronology ranging from 3813 ± 31 a BP to 3068 ± 35 a BP. The content of TOC fluctuated between 33.4% and 49.0%, showing no obvious trends, which implied that the vegetation composition and sedimentary environment stayed stable and kept a rather reductive environment in this region during the period. Because

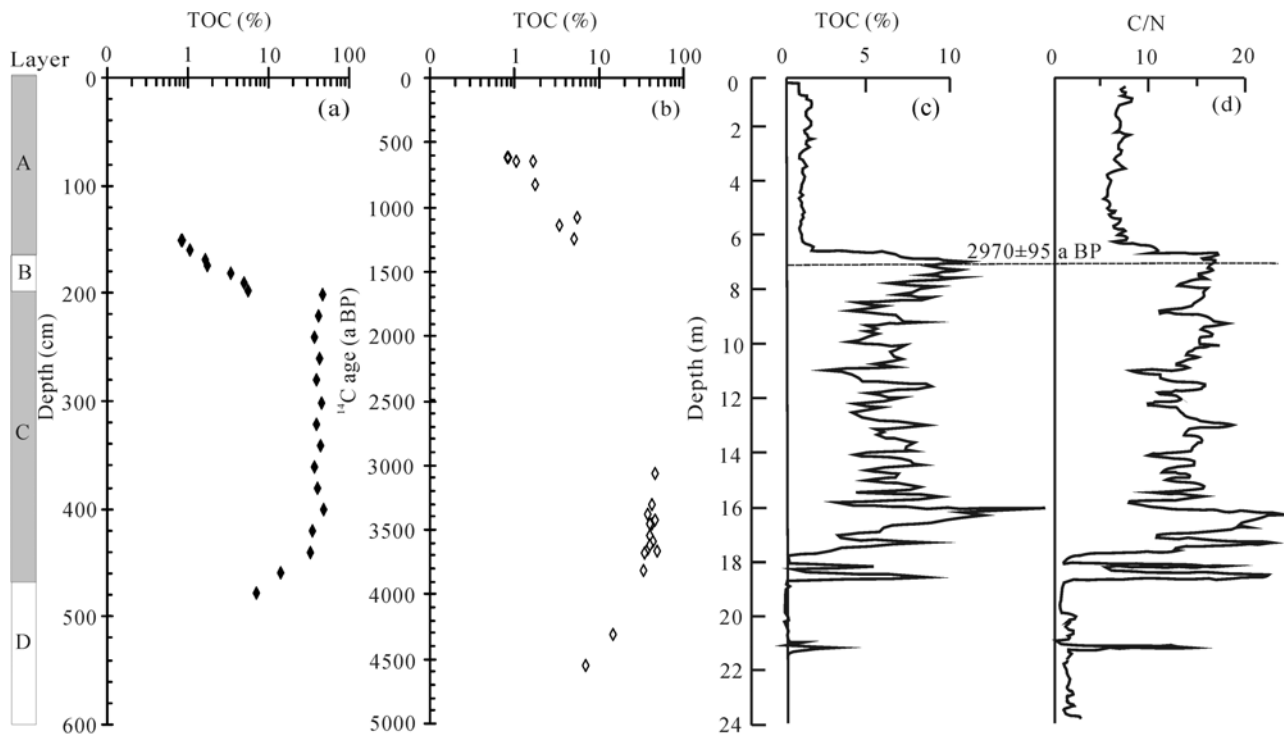


Figure 4 Distribution of TOC content in the sedimentary profile and Shuangchi Maar Lake with C/N ratio. (a), (b) Variation of TOC content with depth and age in the sedimentary profile; (c), (d) variation of TOC content and C/N ratio with depth in Shuangchi Maar Lake in Hainan.

Glyptostrobus pensilis tends to grow along the river bank or in wetland^[22], the region was most likely to be wetland with a warm and wet climate during that period. In layer D, the basement of the ancient forest, the content of TOC decreased from 14.5% to 6.7% from 4544±30 a BP to 3813±31 a BP. Given the combination of the sedimentary property and the probable source of organic carbon, such low content of TOC in layer D could not be formed in the wetland. This suggests that the region could not be a wetland between 4.5 ka BP and 4.2 ka BP and that the wetland should initiate between 4.2 ka BP and 3.8 ka BP.

As shown in Figure 2, the properties of the sediments in layers B and C changed obviously. The change also exhibited in the radiocarbon chronology, the content of TOC and the $\delta^{13}\text{C}$ values, which reflected the distinguished difference of ecological environment before and after 3.0 ka BP. The cause of the great interval of radiocarbon age between layers C and B was possibly linked to the neotectonic movement. Sihui lies in the active region of the neotectonic movement, and vertical activities occurred frequently through Holocene^[23]. When the block was lifted, erosion caused by exogenetic forces would lead to the loss of the stratum between 3068±35 a BP and 1250±29 a BP. In addition, the erosion intensity significantly enhanced around 3.0 ka BP in South China as indicated by the changes of the content of TOC and the ratio of C/N (Figure 4(c) and (d)) in Shuangchi Maar Lake in Hainan^[11].

2.3 Variation of atmospheric CO₂ concentration during 3.5–3.0 ka BP

Many proxies recorded the climatic variation of Holocene^[24–28]. The ice core and stalagmite records are generally acknowledged relatively precise. However, in Pearl River Delta, the main proxies are corals and sediments in lakes^[3,10–11]. Studies on the tree-rings in this region has not been reported yet.

The fine root can record the climate information when it grows. It is the main organ of plant for the water and nutrient absorption, in which the carbon is produced through photosynthesis^[29]. The life span of fine root is short, usually ranging from days to months, years at most^[30–34]. The biomass of fine root tends to concentrate in the litter layer or above 10 centimeters of mineral topsoil, and declines with depth in exponential^[31,35–37]. The $\delta^{13}\text{C}$ value of the fine root is not influenced by

temperature, but mainly controlled by atmospheric CO₂ concentration and the precipitation. Influence of precipitation mainly shows up on the use efficiency of water: high $\delta^{13}\text{C}$ value stands for high use efficiency of water, and the opposite is also true^[38]. Because of the swampy environment, the water use efficiency of the fine root could not be affected significantly. Variation of $\delta^{13}\text{C}$ value of fine root thus shows the variation of atmospheric CO₂ concentration.

Abundant fine roots with different colors and densities are preserved in layer C. In order to assure that all the fine roots belong to the same period, we collected the samples at the same position with the darkest color and diameter less than 0.5 mm from each site. Thus, $\delta^{13}\text{C}$ values of the mixed fine roots would reflect the average $\delta^{13}\text{C}$ values of atmospheric CO₂ when the fine roots grew.

$\delta^{13}\text{C}$ values of fine roots in the profile ranged between –28.60‰ and –27.26‰ with an average value of –27.84‰ (Figure 5(a)). Marshall et al.^[39] presented the relationship between the $\delta^{13}\text{C}$ value of plant ($\delta^{13}\text{C}_p$) and atmospheric CO₂ ($\delta^{13}\text{C}_a$) as follows:

$$\delta^{13}\text{C}_p = \delta^{13}\text{C}_a - a - (b-a)C_i/C_a, \quad (1)$$

a stands for the fractionation factor (4.4‰) caused by the diffusion effect when CO₂ pass stomas of plant. b denotes ¹³CO₂ fractionation value (29‰) when the leaf fix atmospheric CO₂ through photosynthesis^[40]. C_i/C_a represents the ratio between CO₂ content (C_i) in leaves and atmosphere (C_a). For C₃ plant in general, the variation of the atmospheric CO₂ content has litter influence on C_i/C_a ^[41].

In the simulation, we applied the function:

$$\delta^{13}\text{C}_L = \delta^{13}\text{C}_{R.A} - 2.0\text{‰}, \quad (2)$$

where $\delta^{13}\text{C}_L$ stands for the $\delta^{13}\text{C}$ value of *Glyptostrobus pensilis* leaf, and $\delta^{13}\text{C}_{R.A}$ stands for the average $\delta^{13}\text{C}$ value of fine root (–27.84‰). 2.0‰ is the fractional constant of ¹³C between the leaves and fine roots of conifer plants^[29]. The $\delta^{13}\text{C}$ value of atmospheric CO₂ was supposed to be –6.5‰ at that time^[27]. Inputting these data above into eq. (1), we finally got $C_i/C_a = 0.77$. Inputting all the $\delta^{13}\text{C}$ values of fine roots into eq. (3):

$$\delta^{13}\text{C}_{R.A} - 2.0\text{‰} = \delta^{13}\text{C}_a - a - 0.77 \times (b-a). \quad (3)$$

Results are shown in Figure 5(b).

Mook et al.^[42] and Keeling et al.^[43] have found that fine inverse correlation existed between modern atmospheric CO₂ content and $\delta^{13}\text{C}$ values, expressed by eq.

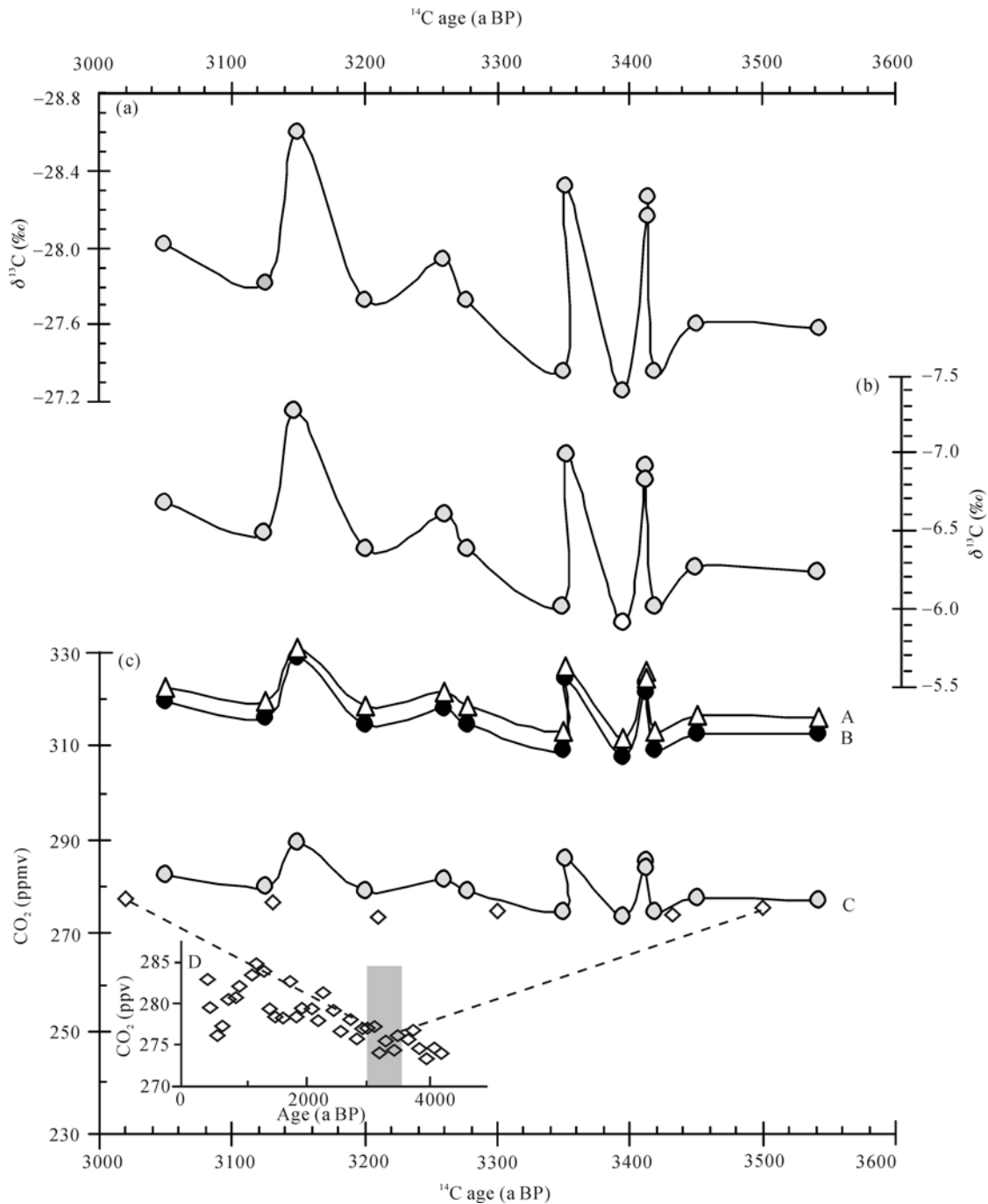


Figure 5 Distribution of the $\delta^{13}\text{C}$ values of fine roots, and simulation results of the atmospheric CO_2 content and the $\delta^{13}\text{C}$ values during 3.5 ka BP to 3.0 ka BP. (a) Variation of $\delta^{13}\text{C}$ values of fine roots with the depth; (b) simulation results of the $\delta^{13}\text{C}$ values of atmospheric CO_2 during 3.5 ka BP to 3.0 ka BP; (c) variation of atmospheric CO_2 content according to different equations and the ice core record of Antarctica. A, B, C and D denote to the simulation results of the eqs. (5), (6), (4) and ice core records in Taylor Dome, Antarctica, respectively. \diamond in the curve C derived from the data of the shadow in curve D.

(4), in which m is a constant, and n denotes the $\delta^{13}\text{C}$ value of plant leaves.

$$[\text{CO}_2] = m / (\delta^{13}\text{C}_a + n). \quad (4)$$

In this paper, $n = \delta^{13}\text{C}_L (-29.84\text{‰})$; m is determined by the atmospheric CO_2 content (280 ppmv, on average) and the $\delta^{13}\text{C}$ value (-6.5‰ , on average) of pre-indus-

try^[44,45], and the calculated result is 6535.2.

The inverse relationship also showed between the paleo-atmospheric CO_2 content and $\delta^{13}\text{C}$ value. CO_2 trapped in the ice core at Taylor Dome, Antarctica, manifested a fine inverse relationship between atmospheric CO_2 content and $\delta^{13}\text{C}$ values during the past 11

ka BP^[27]. In addition, the relationship had been applied to reconstruct the paleo-atmospheric CO₂ content successfully. White et al.^[24] recovered the variation of the atmospheric CO₂ content since 14 ka BP using this relationship, and the results showed great agreement with the records from the ice core.

Based on eqs. (3) and (4), variation of the atmospheric CO₂ content during 3.5 ka BP to 3.0 ka BP was shown in Figure 5(c)-C. In contrast, Figure 5(c)-A and B showed the simulation results of eqs. (5) and (6) given by Keeling et al.^[43] and Amundson et al.^[46]:

$$\delta^{13}\text{C}_a = -26.54 + 6346/(\text{CO}_2), \quad (5)$$

$$\delta^{13}\text{C}_a = -28.773 + 7128.5 \times 1/(\text{CO}_2). \quad (6)$$

Simulation results showed that the $\delta^{13}\text{C}$ values of the atmospheric CO₂ decreased slightly while the content increased during 3.5 ka BP to 3.0 ka BP in this region, reflecting a warming trend. That was consistent with the records in Taylor Dome, Antarctica.

3 The event around 3.0 ka BP and its impact on human activities

The geographical environment in this region changed greatly before and after 3.0 ka BP: from 4.0 ka BP to 3.0 ka BP, the region was a wetland and covered by the ancient forest which was dominated by the hydrophilous plant *Glyptostrobus pensilis*. The climate had a warming trend during that period. At around 3.0 ka BP, the wetland disappeared and the ancient forest was gone, suggesting the geographical environment likely turned dry at that time. Causes for the drought may link to the climate change and the neotectonic movement. Contemporaneous records of pollen data and $\delta^{18}\text{O}$ values of the sediments from lakes in the low latitude areas around the world all implied that the climate changed dramatically at around 3.0 ka BP^[3,11,12,47]. Haug et al.^[48] confirmed that the precipitation in Cariaco Basin, South America, declined sharply at 3.0 ka BP. $\delta^{18}\text{O}$ values of the stalagmite from Dongge Cave also recorded the less precipitation and weaker strength of East Asian Summer Monsoon at that time^[49]. The Titanium content from Huguang Maar Lake in Zhanjiang, near the study area, also displayed the strengthened Winter Monsoon at 3 ka BP. Almost at the same time, the cyclicity and intensity of the ENSO enhanced distinctly, and the ENSO-teleconnected regions were characterized by an increased impact of ENSO^[50]. The ancient forest and wetland were likely to disappear under such climate conditions. Ver-

tical activity of the neotectonic movement could also lead to hydrological changes in this region. However, the ancient forest had been preserved thanks to rapid burial. If the drought was caused by vertical movement, the ancient forest could not have been buried rapidly. Therefore, the reason for the disappearance of the ancient forest was related to climate changes at around 3.0 ka BP.

Acknowledged mechanisms of the climate change around 3.0 ka BP are associated with the changes of monsoon intensity^[51], ENSO activities^[52], North Atlantic current^[53], and the annual position of Intertropical Convergence Zone (ITCZ)^[3,48]. For the East Asia at that time, the climate change is likely to be driven by transition of the annual position of ITCZ. When the ITCZ towards south, the summer monsoon intensity would decline while the winter monsoon intensity will increase, and the North Hemisphere turns dry and cold. In addition, the southward transfer of ITCZ could improve the intensity of ENSO activity^[48]. These are all in agreement with paleoclimate records in this region. Thus, the southward transfer of ITCZ would be the main reason for the climate change in this region.

The climate change around 3.0 ka BP may have greatly impacted on the production and life style of ancient people in this region. Along with the climate change, the sea level decreased^[54,55]. Traditional gathering and fishing could not satisfy the need of life, as a result, agriculture especially rice planting flourished^[4]. Maybe the same reason led to the termination of the Shell Mound Sites and Sand Mound Sites at around 3.0 ka BP in Pearl River Delta.

4 Results

(1) The ancient forest in Sihui began to develop at around 4.0 ka BP, and disappeared at about 3.0 ka BP. The region was a wetland, and climate stayed warm and wet during this period.

(2) The region was dominated by C₃ plant during 4.5 ka BP to 0.6 ka BP, however, the biomass of the surface vegetation declined during 1.2 ka BP to 0.6 ka BP. The organic carbon in layer C almost remained undecomposed.

(3) Simulation results showed that the atmospheric CO₂ content increased slightly during 3.5 ka BP to 3.0 ka BP, consistent with the records of the ice core in Antarctica, indicating a warming trend during the pe-

riod.

(4) Disappearance of the ancient forest and wetland was likely to associate with the drought at around 3.0 ka BP. The southward transfer of ITCZ was possibly the

main mechanism of the climate change.

We are grateful to Prof. Li Pingri and Senior Engineer Tan Huizhong from Guangzhou Institute of Geography, Guangdong Academy of Sciences for their assistance with fieldwork.

- 1 Hodell D A, Curtlis J H, Brenner M. Possible role of climate in the collapse of Classic Maya civilization. *Nature*, 1995, 375: 391–394[DOI]
- 2 Zheng Z, Deng H, Zhang H, et al. Holocene environmental changes in the tropical and subtropical areas of the South China and the relation to human activities (in Chinese). *Quat Sci*, 2004, 24: 387–393
- 3 Yancheva G, Norbert N R, Mingram J. Influence of the intertropical convergence zone on the East Asian monsoon. *Nature*, 2007, 445: 74–77[DOI]
- 4 Weng Q. Human-environment interactions in agricultural land use in a South China's wetland region: A study on the Zhujiang Delta in the Holocene. *Geol J*, 2000, 51: 191–202
- 5 Fang X Q, Zhang W B, Zhang L S. The land use arrangement of China in the Holocene megathermal period and its significance (in Chinese). *J Nat Resour*, 1998, 13(1): 16–22
- 6 Huang G Q. Neolithic culture and paleogeographic environment in the Zhujiang Delta (in Chinese). *Acta Geograph Sin*, 1996, 51(6): 508–517
- 7 Wen X S, Peng Z C, Zhao H T. Advance in study on the Holocene climate evolution in China (in Chinese). *Adv Earth Sci*, 1999, 14: 292–298
- 8 He Y Q, Yao T D, Shen Y P, et al. Climatic differences in China during the Holocene indicated by the various climatic proxy data from different parts of China (in Chinese). *J Glaciol Geocryol*, 2003, 25(1): 11–18
- 9 Yao T D, Yang Z H, Huang C L, et al. A high-resolution climate and environment records in the past 2 ka — Preliminary study of Guliya ice core records. *Chin Sci Bull*, 1996, 41(12): 1103–1106
- 10 Yu K F, Liu D S, Shen C D, et al. High-frequency climatic oscillations recorded in a Holocene coral reef at Leizhou Peninsula, South China Sea. *Sci China Ser D-Earth Sci*, 2002, 45(12): 1057–1067
- 11 Zheng Z, Wang J H, Wang B, et al. High-resolution records of Holocene from Suangchi Maar Lake in Hainan Island. *Chin Sci Bull*, 2003, 48(5): 497–502
- 12 Hodell D A, Curtis J H, Jones G A, et al. Reconstruction of Caribbean climate change over the past 10500 years. *Nature*, 1991, 352: 790–793[DOI]
- 13 Zhu X Y, Zhang M L, Lin Y S, et al. Carbon isotopic records from stalagmites and the signification of paleo-ecological environment in the area of Guangxi-Guizhou, China. *Environ Geol*, 2006, 51: 267–273[DOI]
- 14 Li P R, Cui H T, Tan H Z, et al. A study on Holocene buried timbers in Guangdong (in Chinese). *Tropical Geogr*, 2001, 21(3): 195–197
- 15 Ding P, Shen C D, Yi W X, et al. ^{14}C chronological research of ancient forest ecosystem in Sihui, Guangdong Province (in Chinese). *Quat Sci*, 2007, 27(4): 492–498
- 16 Davidson G R. The stable isotopic composition and measurement of carbon in CO_2 . *Geochim Cosmochim Acta*, 1995, 59: 2485–2489[DOI]
- 17 Bird M I, Chivas A R, Head J A. Latitudinal gradient in carbon turnover times in forest soils. *Nature*, 1996, 381: 143–146[DOI]
- 18 Deines P. The isotopic composition of reduced organic carbon. In: Fritz P, Fontes J C, eds. *Hand Book of Environment Isotope Geochemistry 1: The Terrestrial of Environment*. Amsterdam: Elsevier Science, 1980. 329–406
- 19 Chen Q Q, Shen C D, Sun Y M, et al. Spatial and temporal distribution of carbon isotopes in soil organic matter at the Dinghushan Biosphere Reserve, South China. *Plant Soil*, 2005, 273: 115–128[DOI]
- 20 Shen C D, Beer J, Ivy-Ochs S, et al. ^{10}Be , ^{14}C distribution, and soil production rate in a soil profile of a grassland slope Heshan hilly land, Guangdong. *Radiocarbon*, 2004, 46: 445–454
- 21 Shen C D, Yi W X, Sun Y M, et al. ^{14}C apparent ages and $\delta^{13}\text{C}$ distribution of forest soils in Dinghushan Natural Reserve (in Chinese). *Quat Sci*, 2000, 20(4): 335–344
- 22 Li F G, Xia N H. The geographical distribution and cause of threat to *Glyptostrobus pensilis* (Taxodiaceae) (in Chinese). *J Trop Subtrop Bot*, 2004, 12: 13–20
- 23 Chen W G, Wei B L, Zhao H M, et al. The neotectonic movement in Pearl River Delta area (in Chinese). *South China J Seis*, 2002, 1: 8–18
- 24 White J W C, Ciais P, Figge R A, et al. A high-resolution record of atmospheric CO_2 content from carbon isotopes in peat. *Nature*, 1994, 367: 153–156[DOI]
- 25 Marino B D, McElroy M B. Isotopic composition of atmospheric CO_2 inferred from carbon in C_4 plant cellulose. *Nature*, 1991, 349: 127–131[DOI]
- 26 Archer D, Maier-Reimer E. Effect of deep-sea sedimentary calcite preservation on atmospheric CO_2 concentration. *Nature*, 1994, 367: 260–264[DOI]
- 27 Indermühle A, Stocker T F, Joos F, et al. Holocene carbon-cycle dynamics based on CO_2 trapped in ice at Taylor Dome, Antarctica. *Nature*, 1999, 398: 121–126[DOI]
- 28 Wang Y J, Cheng H, Edwards R L, et al. A high-resolution absolute-dated Late Pleistocene monsoon record from Hulu Cava, China. *Science*, 2001, 294: 2345–2348[DOI]
- 29 Hobbie E A, Tingey D T. Contributions of current year photosynthate to fine roots estimated using a ^{13}C -depleted CO_2 source. *Plant Soil*, 2002, 247: 233–242[DOI]
- 30 Shan J P, Tao D L. Overseas researches on tree fine root (in Chinese). *Chin J Ecol*, 1992, 11(4): 46–49
- 31 Zhang X Q, Wu K H. Fine-root production and turnover for forest ecosystems (in Chinese). *Sci Sil Sin*, 2001, 37(3): 126–138
- 32 Majdi H, Pregitzer K, Morén A S, et al. Measuring fine root turnover in forest ecosystems. *Plant Soil*, 2005, 276: 1–8[DOI]
- 33 Baddeley J A, Watson C A. Influences of root diameter, tree age, soil depth and season on fine root survivorship in *Prunus avium*. *Plant Soil*,

- 2005, 276: 15–22[DOI]
- 34 Black K E, Harbron C G. Differences in root longevity of some tree species. *Tree Physiol*, 1998, 18: 259–264
- 35 Burke M K, Raynal D J. Fine root growth phenology, production, and turnover in a northern hardwood forest ecosystem. *Plant Soil*, 1994, 162: 135–146[DOI]
- 36 Majdi H, Persson H. Spatial distribution of fine roots, rhizosphere and bulk-soil chemistry in an acidified *Picea abies*. *Scandinavian J Forest Res*, 1993, 8: 147–155[DOI]
- 37 Wen D Z, Wei P, Kong G H, et al. Production and turnover rate of fine roots in two lower subtropical forest sites at Dinghushan (in Chinese). *Acta Phytocool Sin*, 1999, 23(4): 361–369
- 38 Farquhar G D, Ehleringer J R. Carbon isotope discrimination and photosynthesis. *Ann Rev Plant Physiol Plant Mol Biol*, 1989, 40: 503–537[DOI]
- 39 Marshall J D, Monserud R A. Homeostatic gas-exchange parameters inferred from $^{13}\text{C}/^{12}\text{C}$ in tree rings of conifers. *Oecologia*, 1996, 105: 13–21[DOI]
- 40 Roeske C A, O' Leary M H. Carbon isotope effect on carboxylation of ribulose biphosphate catalyzed by ribulose biphosphate carboxylase from *Rhodospirillum rubrum*. *Biochemistry*, 1985, 24: 1603–1607[DOI]
- 41 Polley H W, Johnson H B. Increase in C3 plant water-use efficiency and biomass over Glacial to present CO_2 concentration. *Nature*, 1993, 361: 61–64[DOI]
- 42 Mook W G, Koopmans M, Carter A F. Seasonal, latitudinal, and secular variation in the abundance and isotopic ratios of atmospheric carbon dioxide. *J Geophys Res*, 1983, 88: 10915–10933[DOI]
- 43 Keeling C D, Mink W G. Recent trends in the $^{13}\text{C}/^{12}\text{C}$ ratio of atmospheric carbon dioxide. *Nature*, 1979, 277: 121–122[DOI]
- 44 Neftel A, Moor R, Oeschger H, et al. Evidence from polar ice for the increase in atmospheric CO_2 in the past two centuries. *Nature*, 1985, 315: 45–47[DOI]
- 45 Friedli H, Löttscher H, Oeschger H, et al. Ice core record of the $^{13}\text{C}/^{12}\text{C}$ ratio of atmospheric CO_2 in the past two centuries. *Nature*, 1986, 324: 237–238[DOI]
- 46 Amundson R, Stern L, Baisden T, et al. The isotopic composition of soil and soil-respired CO_2 . *Geoderma*, 1998, 82: 83–114[DOI]
- 47 Stott L, Cannariato K, Thunell R, et al. Decline of surface temperature and salinity in the western tropical Pacific Ocean in the Holocene epoch. *Nature*, 2004, 431: 56–59[DOI]
- 48 Haug G H, Hughen K A, Sigman D M, et al. Southward migration of the Intertropical Convergence Zone through the Holocene. *Science*, 2001, 293: 1731–1753
- 49 Dykoski C A, Edwards R L, Cheng H, et al. A high-resolution, absolute-dated Holocene and deglacial Aian monsoon record from Dongge Cave, China. *Earth Planet Sci Lett*, 2005, 233: 71–86[DOI]
- 50 Donders T H, Cremer F W, Visscher H. Integration of proxydata and model scenarios for the mid-Holocene onset of modern ENSO variability. *Quat Sci Rev*, 2008, 27: 571–579[DOI]
- 51 Lamb H F, Gasse F, Benkaddour A, et al. Relation between century-scale Holocene arid intervals in tropical and temperate zones. *Nature*, 1995, 373: 134–137[DOI]
- 52 Moy M C, Seltzer G O, Rodbell D T, et al. Variability of El Niño/Southern Oscillation activity at millennial timescales during the Holocene epoch. *Nature*, 2002, 420: 162–165[DOI]
- 53 Street-Perrott F A, Perrott R A. Abrupt climate fluctuations in the tropics: The influence of Atlantic Ocean circulation. *Nature*, 1990, 343: 607–612[DOI]
- 54 Fang G X, Li P R, Huang G Q. Sea level changes in Zhujiang Delta during the past 8000 years (in Chinese). *Geogr Res*, 1991, 10(4): 1–11
- 55 Zong Y Q. Mid-Holocene sea-level highstand along the Southeast Coast of China. *Quat Int*, 2004, 117: 55–67[DOI]